A Protective Vaccine Delivery System for *In Vivo* T Cell Stimulation Using Nanoengineered Polymer Hydrogel Capsules

Amy Sexton,[†,§] Paul G. Whitney,[†,§] Siow-Feng Chong,[‡] Alexander N. Zelikin,[‡] Angus P. R. Johnston,[‡] Robert De Rose,[†] Andrew G. Brooks,[†] Frank Caruso,[‡,*] and Stephen J. Kent[†,*]

[†]Department of Microbiology & Immunology and [‡]Centre for Nanoscience and Nanotechnology, Department of Chemical and Biomolecular Engineering, The University of Melbourne, Parkville, Victoria 3010, Australia. [§]The authors contributed equally.

ABSTRACT Successful delivery of labile vaccine antigens, such as peptides and proteins, to stimulate CD4 and CD8 T cell immunity could improve vaccine strategies against chronic infections such as HIV and Hepatitis C. Layer-by-layer (LbL)-assembled nanoengineered hydrogel capsules represent a novel and promising technology for the protection and delivery of labile vaccine candidates to antigen-presenting cells (APCs). Here we report on the *in vitro* and *in vivo* immunostimulatory capabilities of LbL-assembled disulfide cross-linked poly(methacrylic acid) (PMA_{SH}) hydrogel capsules as a delivery strategy for protein and peptide vaccines using robust transgenic mice models and ovalbumin (OVA) as a model vaccine. We demonstrate that OVA protein as well as multiple OVA peptides can be successfully encapsulated within nanoengineered PMA_{SH} hydrogel capsules. OVA-containing PMA_{SH} capsules are internalized by mouse APCs, resulting in presentation of OVA epitopes and subsequent activation of OVA-specific CD4 and CD8 T cells *in vitro*. OVA-specific CD4 and CD8 T cells are also activated to proliferate *in vivo* following intravenous vaccination of mice with OVA protein- and OVA peptide-loaded PMA_{SH} hydrogel capsules. Furthermore, we show that OVA encapsulated within the PMA_{SH} capsules resulted in at least 6-fold greater proliferation of OVA-specific CD8 T cells and 70-fold greater proliferation of OVA-specific CD4 T cells *in vivo* compared to the equivalent amount of OVA protein administered alone. These results highlight the potential of nanoengineered hydrogel capsules for vaccine delivery.

KEYWORDS: layer-by layer · hydrogel · nanoengineering · vaccine · delivery · *in vivo* · T cell stimulation

Vaccines are the preferred solution for preventing pathogenic infections; however, traditional vaccine strategies have been unsuccessful in immunizing against many important chronic infectious diseases such as HIV and Hepatitis C (HCV). There are now urgent calls for novel vaccine technologies that are safe and able to deliver the vaccine efficiently to specialized antigen presenting cells (APCs), such as dendritic cells (DCs), to augment the immune response. Insightful chemical and material strategies that address these issues are expected to have a major impact on the control of HIV/AIDS as well as being applicable to many other devastating infectious diseases.

In the case of HIV, considerable evidence suggests that T cell immunity can exert some control over viremia.[1] Although CD8 T cells are directly responsible for killing virus-infected cells, CD4 T cells play a critical role in inducing and maintaining the functionality of this cytotoxic T lymphocyte (CTL) response. Therefore, these helper CD4 T cells are considered to potentially play an important role in the control of HIV[2,3] and HCV infections.[4] Hence, vaccines that induce broad CD4 and CD8 T cell responses are more likely to be successful at controlling such chronic viral infections.

Peptides derived from the Gag protein of HIV make safe vaccine antigens and are able to stimulate high levels of both CD4 and CD8 T cell immunity and slow the progression of AIDS in a monkey model when pulsed *ex vivo* on blood cells prior to intravenous administration.[5] However, peptides administered without prior *ex vivo* pulsing are poorly immunogenic and rapidly degrade *in vivo* by blood proteases.[6] In order to develop peptides as vaccines, novel delivery techniques are required to protect antigens and efficiently deliver them to APCs *in vivo*.

Encapsulation techniques have recently been pioneered to deliver therapeutic agents *in vivo*. A number of techniques can be used for encapsulation, including micelles,[7] liposomes,[8] polymersomes,[9,10] and nanoengineered layer-by-layer (LbL) capsules.[11,12] We recently developed LbL capsules for encapsulating peptide vaccines.[13,14] These capsules are prepared by the LbL deposition of interacting polymers onto a colloidal template that is

*Address correspondence to skent@unimelb.edu.au, fcaruso@unimelb.edu.au.

Received for review July 1, 2009 and accepted October 5, 2009.

Published online October 13, 2009.
10.1021/nn900715g CCC: $40.75

subsequently removed. The fine control over size and composition and loading makes LbL capsules advantageous for vaccine formulations, allowing reliable dosage and standardized reproducible manufacture. Furthermore, for protein and peptide vaccine delivery, not only can the encapsulation process protect the vaccines from degradation (ensuring the delivery of a high payload of antigen to APCs) but, in addition, the particulate nature of the capsules makes them subject to phagocytosis by professional APCs and macropinocytosis by DCs, thereby delivering the vaccine to key cells that initiate immune responses.[15] Furthermore, these capsules are biodeconstructible, as they are assembled from poly(methacrylic acid) (PMA)-modified with thiol groups (PMA_{SH}).[16] Conversion of the thiol groups into stabilizing disulfide linkages between the polymer layers ensures that the PMA_{SH} capsules remain stable in the oxidative extracellular environment. However, when the capsules are in a reducing environment, such as inside the cell, the capsules are expected to degrade and facilitate the release of the vaccine cargo.[17] We recently demonstrated that peptide-loaded PMA_{SH} hydrogel capsules are readily internalized by human blood APCs to activate peptide-specific CD8 T cell responses *in vitro*.[13,14] Although these *in vitro* studies demonstrate the promise of this technology, the utility of these capsules for the delivery of vaccines *in vivo*, as well as their ability to stimulate both CD4 and CD8 T cell responses to cause rapid activation and proliferation, has yet to be shown.

Here we report on the *in vivo* immunostimulatory capabilities of polymer hydrogel capsules loaded with protein or peptides. Using PMA_{SH} hydrogel capsules assembled by the LbL method, we have encapsulated either whole ovalbumin (OVA) protein or multiple immunogenic OVA peptides as a model vaccine. We assessed their immunogenicity using well-defined mouse models, taking advantage of two existing T cell receptor transgenic mouse strains: OT-I mice which have CD8 T cells that uniquely recognize a specific OVA peptide (SIINFEKL, $OVA_{257-264}$) restricted by MHC- I ($H2\text{-}K^b$)[18] and OT-II mice which have CD4 T cells specific for the OVA peptide ISQAVHAAHAEINEAGR ($OVA_{323-339}$) restricted by MHC-II ($I\text{-}A^b$).[19] Using these transgenic mice models, we assessed the capacity of OVA proteins and peptides encapsulated within PMA_{SH} hydrogel capsules to be intracellularly processed and presented for T cell recognition and subsequent proliferation. We show that OVA proteins/peptides delivered by capsules stimulate T cell immunity more effectively than OVA protein administered alone. These results demonstrate the *in vivo* potential of this novel capsule-based vaccine delivery technology.

RESULTS

LbL Capsule Assembly, Loading, and Release. We previously described the LbL assembly of single-component PMA hydrogel capsules stabilized *via* disulfide linkages and demonstrated their high colloidal stability and monodisperse size preparation.[17] Such features make these capsules well-suited to serve as drug carriers.[20] To this end, we have developed methods to load these capsules with therapeutic molecules such as single- and double-stranded DNA[21] and oligopeptide sequences.[13] Confinement of cargo within polymer hydrogel capsules is achieved by immobilizing the therapeutic onto the surface of a template particle followed by assembly of the polymer thin film and subsequent removal of the core particle (Figure 1a). We have demonstrated that cargo encapsulation relies on both size exclusion and electrostatic repulsion provided by the negatively charged polymer capsule wall.[14] Previously, encapsulation of whole proteins within polyelectrolyte capsules (including PMA_{SH}) has been achieved using porous silica templates.[16,22] Herein, we investigate the encapsulation of whole OVA protein ($M_W = 45$ kDa, 385 amino acids) by surface immobilization on solid silica particles using a similar method we previously reported to encapsulate oligonucleotides.[21]

To determine the efficiency of whole OVA protein adsorption on the surface of the nonporous silica templates, the OVA was fluorescently labeled, and the fluorescence of the particles and the solution was measured. At low OVA concentrations (<1 fg per particle), limited fluorescence was observed in the adsorption solution, indicating close to 100% efficiency of adsorption onto the particles. At higher OVA concentrations (>50 fg per particle), the adsorption efficiency decreased to ~50% (Figure 1b). Flow cytometric analyses of the particles demonstrated saturation of OVA adsorption at concentrations above 50 fg per particle. While saturation of the signal occurs at this point, it is probable that additional OVA is adsorbed to the surface of the particle at higher concentrations, as the higher packing density of the OVA can cause fluorescent quenching. Our previous work involving the encapsulation of DNA[21] has demonstrated that subsaturation surface coverage of the particles (~50%) is required to ensure homogeneous assembly of the subsequent polymer layers. Accordingly, we used a loading concentration of 28 fg of OVA per particle (1 μm diameter) to provide efficient adsorption onto the particles while still enabling homogeneous assembly of the PMA_{SH} polymer film. Sequential deposition of polymer layers and subsequent core removal resulted in stable capsules with confined proteins (Figure 1c).

Successful confinement of small oligopeptides requires anchoring by conjugation to a negatively charged polymer *via* a biodegradable disulfide linkage.[14] This all-aqueous encapsulation method affords the loading of typically $\sim 3 \times 10^5$ and 5×10^4 oligopeptide copies per 1 μm and 500 nm diameter capsules, respectively, and presents no inherent limitations on the encapsulation of multiple peptide sequences. Hence,

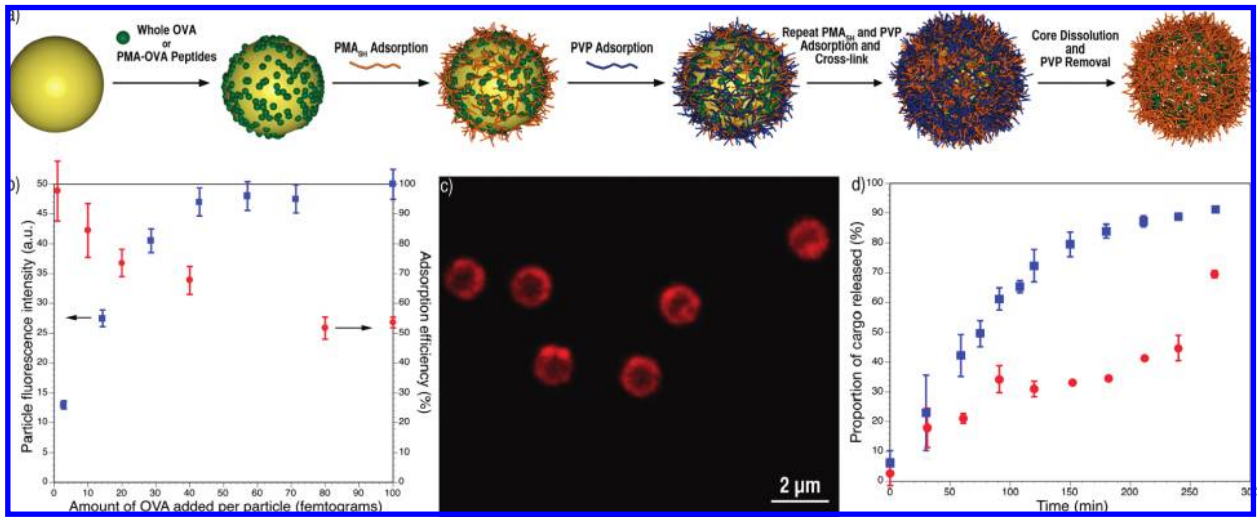

Figure 1. Assembly, loading, and release profiles of whole OVA protein- and OVA peptide-loaded capsules. (a) Schematic illustrating the LbL assembly process. A solid core particle is used to adsorb the protein/peptide vaccines, and alternating layers of interacting polymers (PMA_{SH} and PVP) are subsequently deposited. The solid core is dissolved, and PVP layers are removed to result in the encapsulation of the cargo within the single-component PMA_{SH} hydrogel capsule. (b) Efficiency of OVA adsorption onto the solid silica core particle demonstrating an increase in fluorescence intensity of the particles as OVA is adsorbed (blue squares) and the efficiency of adsorption (red circles, measured by the fluorescence intensity of the remaining solution). Results are the mean and standard deviation (SD) of three samples. (c) Confocal laser scanning microscopy (CLSM) image showing monodisperse OVA-containing capsules (1 μm diameter). (d) Cargo release kinetics of the capsules containing OVA protein (red circles) and OVA peptides (blue squares) under reducing conditions (5 mM GSH). Results are the mean and SD of three experiments.

here we also investigated the coencapsulation of two immunogenic OVA peptides ($OVA_{257-264}$ and $OVA_{323-339}$) within PMA_{SH} capsules. OVA peptides were conjugated to PMA_{SH} anchoring polymers and encapsulated by coadsorption onto solid silica particles as described above.

PMA hydrogel capsules are stabilized through disulfide linkages, which are degraded in the presence of a natural reducing agent, glutathione (GSH).[17] The kinetics of this process may depend on a number of factors, such as the number of deposited polymer layers and the degree of PMA thiolation. We previously showed that a 5 mM solution of GSH results in complete disintegration of PMA hydrogel capsules within 5 h.[17] Anchoring of the OVA peptides within the capsules is also achieved using the thiol−disulfide interconversion; however, this polymer−peptide conjugation involves a single disulfide linkage. Hence, in a 5 mM solution of GSH, the release of OVA peptides from the anchoring polymer precedes complete degradation of the capsules, resulting in the release of approximately 75% of the cargo peptides in 2 h (Figure 1d). In contrast, encapsulated whole OVA protein is gradually released in response to the introduced GSH, possibly due to increased swelling of the capsules[17] and their enhanced permeability. Approximately 40% of the OVA cargo was released over 4 h (Figure 1d), and complete release of the OVA occurred upon disintegration of the capsules. It is important to note that the oxidized, dimeric form of glutathione, GSSG, which is an abundant component of blood, also causes minor release of the encapsulated cargo,[14] which can potentially interfere with the immunological evaluation of PMA capsules. Therefore, to overcome this, capsules were incubated with 5 mM GSSG and subsequently washed into phosphate buffered saline prior to performing the immunological experiments outlined below.

Uptake and Internalization of Capsules by APCs. To determine the feasibility of using PMA_{SH} hydrogel capsules to deliver vaccines in murine models, we first assessed the ability of the capsules to associate with murine APCs *in vitro* by incubating spleen derived mouse cells (splenocytes) for 1 h at 37 °C with 1 μm diameter capsules containing fluorescently labeled OVA protein. The splenocytes were surface stained in order to identify B cells, neutrophils, and DCs, and binding of the capsules to these cell types was assessed by flow cytometry. The OVA-loaded capsules bound to a variety of cell types including conventional splenic DCs (B220-, GR1-, CD11c+), although more binding was observed to CD11b+ DCs compared to CD11b- DCs (Figure 2a), possibly due to the greater abundance of this DC subtype in the spleen. OVA-loaded capsules were also able to bind to splenic plasmacytoid DCs (pDCs), B cells, and to a lesser extent neutrophils (Figure 2b). Confocal laser scanning microscopy (CLSM) experiments confirmed that the observed capsule/DC associations resulted from capsule internalization and not just surface binding (Figure 2c).

***In Vitro* Stimulation of CD8 and CD4 T Cells by OVA-Loaded Capsules.** The binding and internalization of the capsules by APCs in the spleen demonstrates that this approach has potential for vaccine delivery. However, in order to generate a T cell immune response, the protein cargo must be released from the capsules, processed into peptide epitopes, and trafficked for presen-

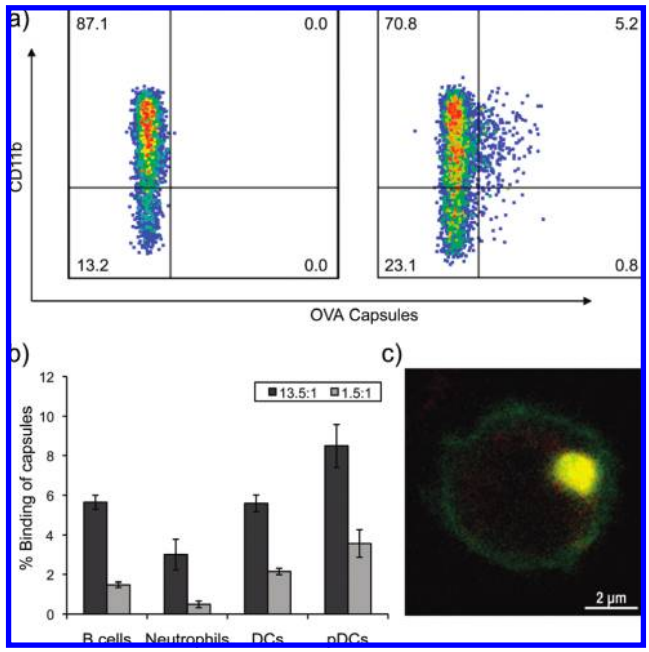

Figure 2. Binding and internalization of OVA-loaded capsules by mouse splenic APCs. Fluorescently labeled OVA was incorporated into PMA_{SH} hydrogel capsules and incubated *in vitro* with mouse splenocytes for 1 h. Association of the capsules with APCs was determined by flow cytometry. (a) DCs identified by antibody staining (CD11c+, GR1-, B220-, CD11b±) with (right panel) and without (left panel) incubation with OVA-loaded capsules at a capsule to cell ratio of 1.5:1. (b) Association of fluorescently labeled OVA-loaded capsules by different splenic cell types (% of cells with capsules bound). Capsules were incubated at a capsule to cell ratio of 13.5:1 and 1.5:1. Cells were identified by surface staining; B cells; B220+ and GR1-, neutrophils; B220-, GR1+, CD11c-, DCs; B220-, GR1-, CD11c+, pDCs; B220+, GR1+, CD11c+. Results are the mean and SD of three different mice spleens. (c) CLSM image demonstrating internalization of fluorescently labeled OVA-loaded capsules (yellow) by mouse spleen derived enriched DCs. Capsules were incubated at a capsule to cell ratio of 100:1, and DCs were identified by surface staining for CD11c (green).

tation with MHC-I and MHC-II molecules and subsequent recognition, activation, and proliferation of cognate CD8 and CD4 T cells. To investigate this, we used existing OVA transgenic mouse models and monitored the proliferation of T cells from transgenic OT-I and OT-II mice to assess presentation of the capsule cargo by murine APCs. OVA protein-loaded capsules were preincubated with APCs and then cocultured with fluorescently labeled transgenic OVA-specific CD8 or CD4 T cells to evaluate their ability to proliferate in response to OVA delivered by the capsules. Incubation of enriched splenic DCs and splenocytes with OVA-loaded capsules at a capsule to cell ratio of 100:1 resulted in the proliferation of more than 80% of both CD4 (OT-II) and CD8 (OT-I) T cells (Figure 3a). This response is comparable to the proliferation induced by 50 μg of soluble OVA protein (25 times more than that delivered with the OVA-loaded capsules). Indeed, APCs incubated with OVA-loaded capsules at a ratio of 100:1 substantially augmented CD4 and CD8 T cell proliferation compared to incubation with 2 μg of OVA protein, equivalent to the OVA protein amount from 100 capsules to 1 splenocyte or 1000 capsules to 1 enriched DC (Figure 3b−e). Each of three repeated experiments showed more proliferating CD4 and CD8 T cells in response to the capsules. There was a median 23 001 more proliferating CD8 T cells (range 9054−58 065 cells) in response to OVA-containing capsules than the equivalent amount of OVA protein, representing a 3.8−7.9-fold increase. Similarly, there was a 5.7−42-fold increase in the numbers of CD4 T cells proliferating in response to OVA capsules compared to the OVA protein controls. Incubation of APCs with empty capsules or media alone did not result in significant CD8 or CD4 T cell proliferation, indicating that T cell proliferation is OVA-specific (Figure 3). In addition, we used OVA peptides that are specifically recognized by the OT-I and OT-II cells as a positive and negative control for each assay. These peptides can bind directly to MHC-I/II on the cell surface without the requirement for antigen processing to activate OT-I CD8 and OT-II CD4 T cells. As expected, the MHC-I epitope ($OVA_{257-264}$) resulted in the proliferation of OT-I CD8 T cells but not OT-II CD4 T cells and *vice versa* for the MHC-II epitope ($OVA_{323-339}$), further demonstrating the specificity of the OT-I and OT-II models.

Stimulation of CD8 and CD4 T Cells *In Vivo*. To assess the immunogenicity of the PMA_{SH} hydrogel capsules *in vivo*, we investigated the proliferation of transgenic OT-I CD8 and OT-II CD4 T cells adoptively transferred into syngeneic mice in response to vaccination of the mice with OVA protein-loaded capsules. Both 1 μm and 500 nm diameter capsules induced the proliferation of at least 85% of adoptively transferred CD4 and CD8 T cells (Figure 4a,b), similar to the proliferation observed in mice vaccinated with OVA-coated splenocytes that included the potent adjuvant lipopolysaccharide (LPS), used as a positive control in order to generate a robust T cell response. Mice vaccinated with OVA-loaded capsules resulted in the proliferation of CD4 T cells at least equivalent to that observed in mice vaccinated with LPS adjuvanted OVA-coated splenocytes (Figure 4d). Indeed, CD4 proliferation was significantly higher in mice vaccinated with 1 μm OVA-loaded capsules compared to mice vaccinated with LPS adjuvanted OVA-coated splenocytes ($p = 0.03$, unpaired t test). Differential proliferative capabilities of the differently sized OVA-loaded capsules are likely due to a dose effect as 500 nm capsules have a 4-fold lower loading capacity compared to the 1 μm capsules. CD8 T cell proliferation was also clearly induced by OVA-loaded capsule vaccination, although to a lesser extent than the mice vaccinated with LPS adjuvanted OVA-coated splenocytes.

Mice vaccinated with PMA_{SH} hydrogel capsules containing the OVA peptides specific for OT-I and OT-II T cells also resulted in marked proliferation of adoptively transferred CD4 T cells and, to a lesser extent, CD8 T cells (Figure 4). Indeed, CD4 T cell proliferation resulting from vaccination with 1 μm diameter capsules containing OVA peptides was more than 10-fold above

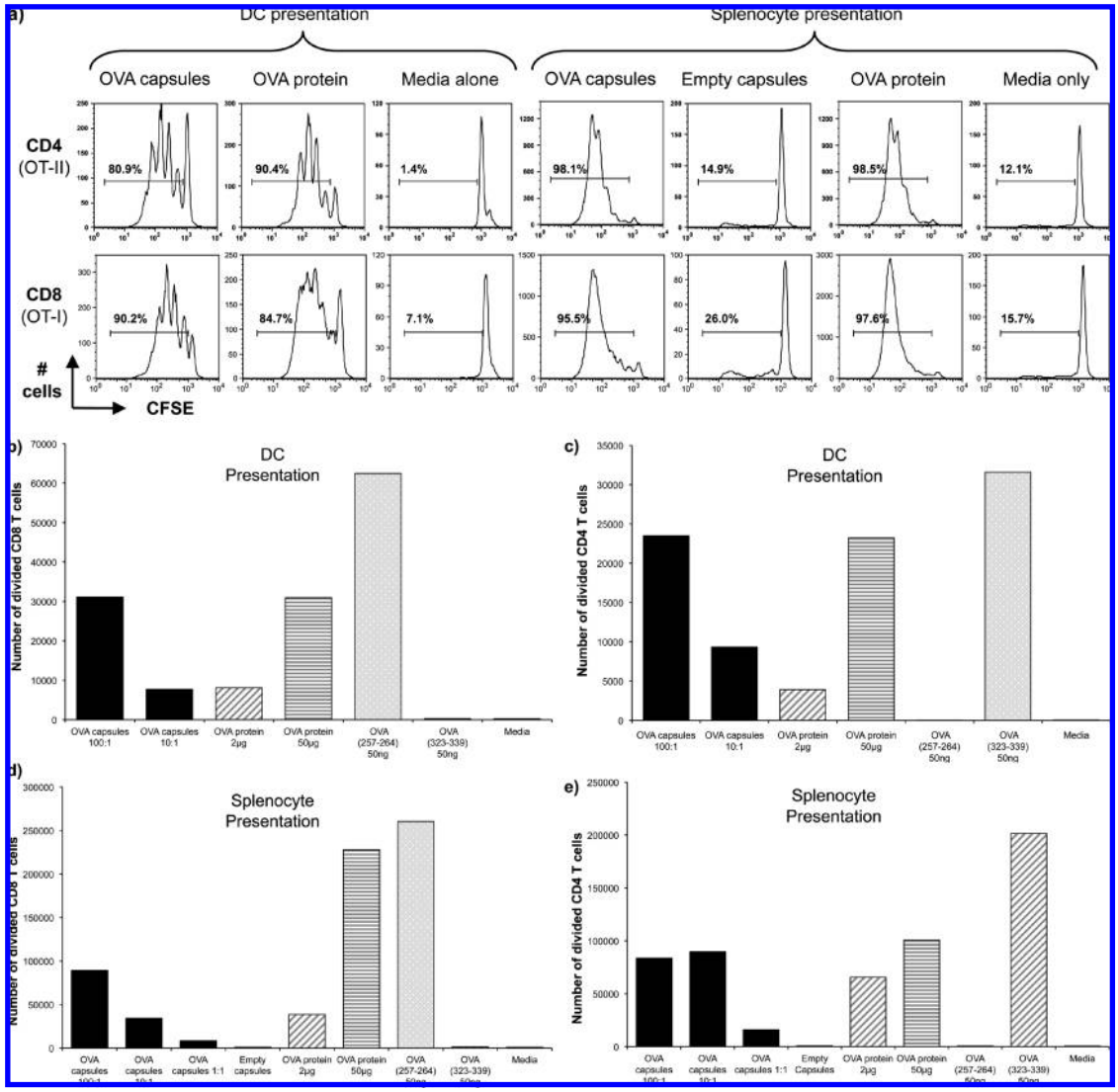

Figure 3. ***In vitro*** **proliferation of CD4 (OT-II) and CD8 (OT-I) T cells in response to presentation of encapsulated OVA by splenic APCs. Enriched DCs (1×10^5) or splenocytes (1×10^6) were preincubated with OVA-loaded capsules before adding CFSE-labeled CD4 (OT-II) or CD8 (OT-I) T cells. T cell proliferation was assessed by diffusion of the CFSE label by flow cytometry after 3 days. (a) Representative flow histograms demonstrating diffusion of the CFSE signal on proliferated CD4 and CD8 T cells in response to OVA presentation by enriched DCs and splenocytes. Graphs show OVA-loaded capsules incubated at a capsule to cell ratio of 100:1. Fifty micrograms of OVA protein was used as a positive control, and empty PMA_{SH} hydrogel capsules (30:1 capsule to cell ratio) and media only included as negative controls. (b−e) Total number of divided T cells in response to OVA presentation by mouse splenocytes or DCs enriched from splenocytes. OVA-loaded capsules were incubated with cells at different capsule to cell ratios (100:1, 10:1, and 1:1). Empty capsules (30:1 capsule to cell ratio) and media only were included as negative controls. Fifty micrograms of OVA protein was included as a positive control alongside the specific OVA peptides recognized by OT-I and OT-II T cells ($OVA_{257-264}$ and $OVA_{323-339}$). OVA protein (2 μg) equivalent to that within 1×10^8 OVA-loaded capsules was also included for comparison. Results are representative of three experiments with three different batches of OVA-loaded capsules.**

that induced from vaccinating with LPS adjuvanted OVA-coated splenocytes; this was found to be significantly higher in an unpaired *t* test ($p = 0.003$) (Figure 4d). The limited CD8 T cell proliferation induced from OVA peptide-loaded capsules may be caused by the susceptibility of the MHC-I restricted OVA peptide to proteolytic degradation,[23] and this may cause this epitope to be degraded before it has a chance to reach the endoplasmic reticulum for MHC-I complexing, hence preventing efficient presentation resulting in limited CD8 T cell stimulation.

In order to demonstrate the ability of the PMA_{SH} hydrogel capsules to more efficiently deliver the protein cargo to APCs, we vaccinated mice with the same amount of whole soluble OVA protein as was administered within the OVA protein-loaded capsules. In these experiments, mice vaccinated with OVA-loaded capsules induced significantly higher CD4 and CD8 T cell proliferation compared with administering the equivalent amount of soluble OVA ($p = 0.0003$ and 0.005 respectively, unpaired *t* test). Indeed, administering the equivalent amount of soluble OVA induced limited pro-

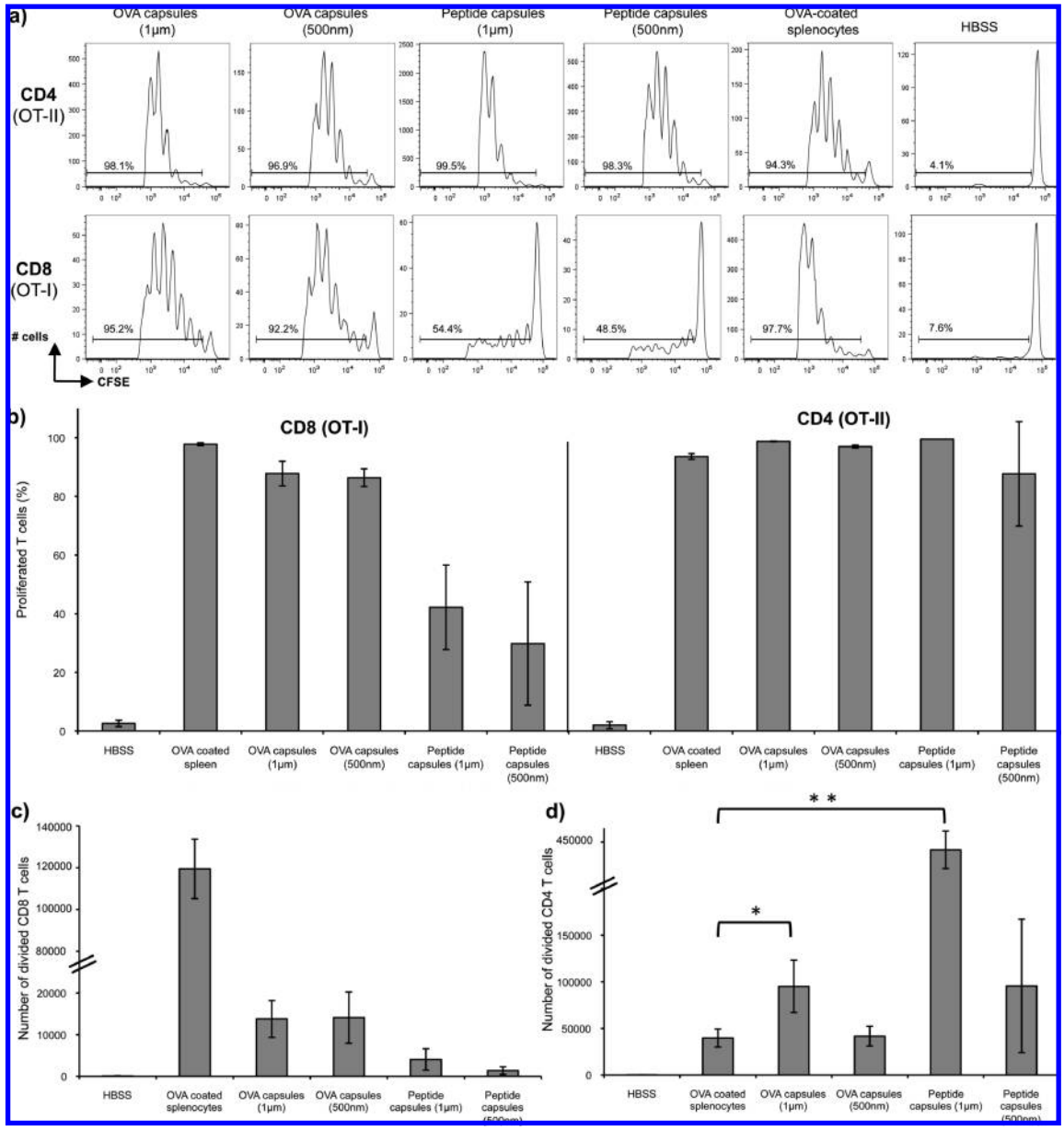

Figure 4. Proliferation of adoptively transferred CD8 (OT-I) and CD4 (OT-II) T cells *in vivo* after OVA-loaded capsule vaccination. OT-I CD8 and OT-II CD4 T cells were CFSE labeled and infused into mice 24 h prior to intravenous vaccination. PMA_{SH} hydrogel capsules containing OVA and OVA peptides were matched for antigen content and administered to groups of three mice. Vaccination of groups of three mice with LPS-adjuvanted OVA-coated splenocytes and Hanks balanced salt solution (HBSS) were used as positive and negative controls, respectively. Proliferation of adoptively transferred CD8 and CD4 T cells in the spleens were examined by flow cytometry after 3 days. (a) Representative flow histograms to show diffusion of the CFSE signal on proliferated adoptively transferred CD4 and CD8 T cells in mice vaccinated with 1 μm and 500 nm diameter capsules containing OVA or OVA peptides. (b) Percentage of proliferated CD8 and CD4 T cells in each vaccinated group of mice. Results show the mean and SD of three mice. (c) Total number of divided CD8 T cells. (d) Total number of divided CD4 T cells. Results show the mean and SD of three mice.

liferation of CD4 and CD8 T cells, whereas OVA encapsulated within 500 nm diameter capsules stimulated high levels of T cell proliferation (>85%, Figure 5a) and generated a mean of 6-fold more divided CD8 T cells and nearly 70-fold more divided CD4 T cells (Figure 5b,c).

DISCUSSION

Vaccine strategies that efficiently target APCs and generate robust and broad cellular immune responses are urgently required to impact viral diseases such as HIV. Nanoengineered polymer hydrogel capsules represent an innovative platform for the protection of proteins and peptides for more efficient delivery to APCs and stimulation of T cell immunity. We show here that (a) multiple peptide antigens can be successfully encapsulated using the PMA_{SH} hydrogel capsule system; (b) capsules are internalized by mouse APCs, including DCs; (c) encapsulated OVA is intracellularly processed by mouse APCs and presented by MHC-I and MHC-II mol-

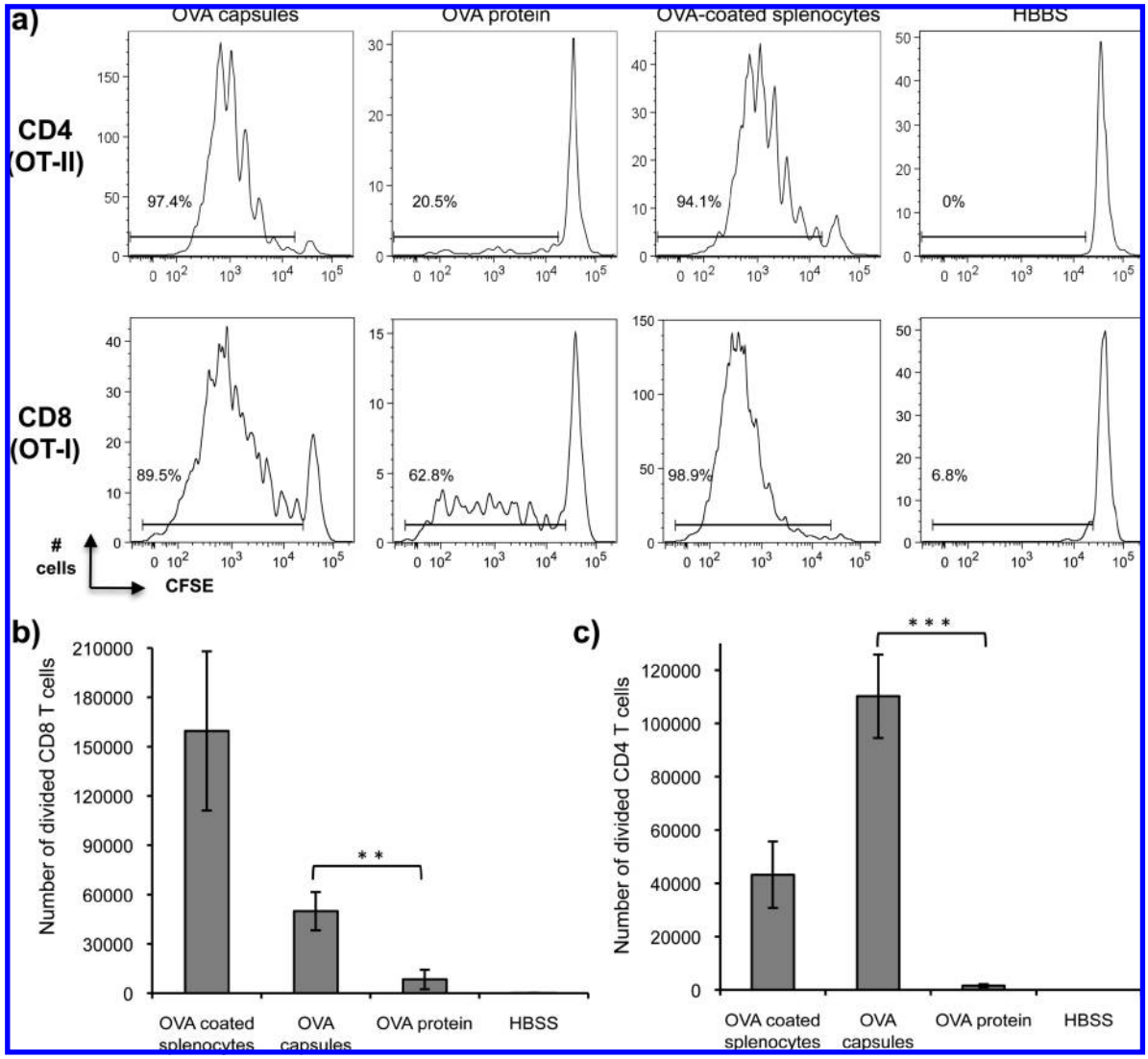

Figure 5. Comparison of CD8 (OT-I) and CD4 (OT-II) T cell proliferation *in vivo* after vaccinating with OVA-loaded capsules or whole OVA alone. CFSE labeled OT-I CD8 and OT-II CD4 T cells were adoptively transferred into mice 24 h prior to intravenous vaccination. Groups of three mice were vaccinated with either 500 nm diameter OVA-loaded capsules or an equivalent amount of soluble OVA for comparison. Vaccination with LPS adjuvanted OVA-coated splenocytes and HBSS were used as positive and negative controls, respectively. Proliferation of adoptively transferred CD8 and CD4 T cells in the spleens were examined by flow cytometry 3 days after vaccination. (a) Representative flow histograms to show proliferation of the adoptively transferred T cells by diffusion of the CFSE signal. (b) Total number of divided CD8 T cells. (c) Total number of divided CD4 T cells. Results show the mean and SD of three mice.

ecules to activate OVA-specific CD4 and CD8 T cells; and (d) encapsulated OVA is more effectively delivered to APCs and results in improved proliferative T cell responses compared to OVA administered alone. These results demonstrate the *in vivo* capabilities of this novel vaccine delivery technology to stimulate robust T cell immunity.

A critical advantage of this delivery technology is the ability to protect antigens for release only once within the cell. We found, both *in vitro* and *in vivo*, that substantially less protein or peptide antigen is required within PMA_{SH} hydrogel capsules compared to free protein antigen to stimulate an equivalent immune response. Ultimately, this means that lower amounts of vaccine antigens will be required for vaccinations using this encapsulation technology; this "dose-sparing" ability of encapsulated vaccines should enable a higher effective dose to be administered with a lower amount of vaccine antigen.

The use of nano- and microparticles for vaccine delivery has been widely explored and evaluated for immunogenicity. For example, biodegradable PLGA particles used to entrap OVA were found to induce higher levels of IFN-γ (a maker for T cell activation) compared to soluble OVA alone when incubated with mouse DCs and OT-I CD8 T cells.[24] Furthermore, Standley *et al.* demonstrated the enhanced proliferation of adoptively transferred OT-I CD8 T cells in mice vaccinated subcutaneously with polyacrylamide particles containing OVA compared to mice vaccinated with soluble OVA alone.[25]

This study[25] also demonstrated enhanced IFN-γ production and cytolytic ability that was further enhanced by the incorporation of CpG, a known adjuvant. The work presented here demonstrates for the first time the induction of T cell proliferation by vaccination with PMA_{SH} hydrogel capsules, indicating that these capsules are an immunogenic system for the protection and delivery of antigens to APCs. Future studies suggested by this work are to investigate the functionality and durability of the T cell responses detected. Furthermore, there is scope to optimize the CD8 T cell immune response induced, which could be achieved by including co-stimulatory molecules to adjuvant the response. Additionally, lysosomal escape peptides could be incorporated. These small peptides will facilitate the disruption of the phagocytic lysosome to improve the bioavailability of the vaccine cargo to the cytosol, hence enabling more efficient MHC-I processing and subsequent CD8 T cell stimulation.

The flexibility of LbL capsule assembly offers enormous possibilities for fine-tuning capsules to augment durable and functional immune responses.[26] Here we have begun to investigate modifications in size and loading of the PMA_{SH} hydrogel capsules. Capsules of both 1 μm and 500 nm in diameter induced proliferation of CD4 and CD8 T cells, although 1 μm capsules were more efficient. This is likely due to the dose effect of differential loading capacities: the 500 nm core templates used for assembly of these capsules comprise a quarter of the surface area available for antigen adsorption compared to the 1 μm capsules. We have also demonstrated the potential for the coencapsulation of multiple peptides, and this method can be used to also incorporate the aforementioned adjuvant molecules and lysosomal escape peptides to further enhance T cell responses. In addition, we are now investigating the possibility of incorporating targeting moieties onto the surface of the capsules to specifically target APCs such as DCs. This is expected to increase specific uptake of the capsules and offers the potential to reduce unwanted adverse reactions and stimulate more durable immunity.

In conclusion, LbL-assembled PMA_{SH} hydrogel capsules are immunogenic vaccines in mice. PMA_{SH} hydrogel capsules warrant further evaluation for use as antigen delivery vehicles to both MHC-I and MHC-II pathways for the induction of durable and functional T cell responses *in vivo*.

METHODS

PMA—OVA Peptide Conjugate Preparation. All materials were purchased from Sigma-Aldrich unless stated otherwise. Poly(methacrylic acid) with 5 mol % of carboxyl groups converted to thiol groups (PMA_{SH}) was synthesized from PMA (M_W = 15 kDa, Polysciences (USA)) and cystamine dihydrochloride *via* carbodiimide coupling, as previously described.[16] The thiol content in the resulting polymer was characterized using Ellman's reagent and a cysteamine standard curve.[27] HiLyte Fluor 488 labeled, cysteine-modified $OVA_{257-264}$ and $OVA_{323-339}$ peptides (synthesized by AnaSpec Inc.) were individually conjugated to Ellman's reagent activated PMA_{SH} (5 mol % carboxyl groups converted to thiol groups) through a disulfide linkage *via* thiol—disulfide exchange. Briefly, sodium borohydride (1 M final concentration) was added to PMA_{SH} (5 mol % carboxyl groups converted to thiol groups, at 10 mg mL^{-1} in water) and incubated at room temperature for 2 h. The reaction was neutralized with concentrated hydrochloric acid, supplemented with K_2HPO_4 (final concentration 0.1 M), and the pH adjusted to 8. Excess Ellman's reagent was added, and the reaction was allowed to proceed for 30 min before purifying by size exclusion chromatography on NAP-25 desalting columns and freeze-drying. The resulting activated PMA_{SH} (PMA_{ER}, 0.632 mg, 0.106 μmol) was dissolved in 95 μL of Tris-EDTA buffer (10 mM, pH 7.5) and combined with a solution of $OVA_{257-264}$ or $OVA_{323-339}$ (0.212 μmol) in nonbuffered water (5 μL). The mixture was incubated overnight with constant mixing and then purified on a NAP-5 desalting column before freeze-drying. The OVA peptide content on each PMA chain was characterized by measuring the release of the 2-nitro-5-mercaptobenzoic acid (TNB) chromophore (λ_{max} = 412 nm) from the polymer by using UV—vis spectrophotometry.

Fluorescent OVA Preparation. OVA was fluorescently labeled with either 5-carboxytetramethylrhodamine, succinimidyl ester (TAMRA), or AlexaFluor-488, succinimidyl ester (Invitrogen). Twenty milligrams of OVA was dissolved in 500 μL of Tris-EDTA buffer and mixed with either 1 mg of TAMRA or 0.1 mg of AlexaFluor-488 dissolved in 10 μL of DMSO. The reaction was allowed to proceed for 2 h at room temperature. The unreacted fluorescent dye was removed by washing the sample 10 times using a 30 000 M_W spin column (Pall Corp) spinning at 10 000*g* for 8 min. The OVA concentration was measured by UV—vis spectrophotometry at 280 nm.

PMA_{SH} Preparation. PMA with 12 mol % carboxyl groups converted to thiol groups for the capsule layers was synthesized from a 299 mg PMA solution (30 wt % solution, Polysciences (USA)) diluted in 5.5 mL of phosphate buffer (0.1 M; pH 7.2). The resulting solution was charged with *N*-(3-dimethylaminopropyl)-*N*′-ethylcarbodiimide (EDC, 64.7 mg) and stirred for 5 min. Subsequently, 45.3 mg of aminoethyl 2-pyridyl disulfide (PDA, SpeedChemical Corp. (China), target modification = 24.5 mol %) was added and incubated at room temperature overnight. The reaction mixture was purified with a 12 kDa dialysis tube and freeze-dried to obtain a white powder of activated PMA_{SH} (PMA_{PD}). The thiol content in the resulting polymer was characterized using dithiothreitol (DTT) and a PDA standard curve (by measuring the release of 2-pyridinethione (λ_{max} = 343 nm)). PMA_{PD} was incubated in a 0.5 M solution of DTT in MOPS buffer (20 mM; pH 8) at a concentration of 100 mg mL^{-1} for at least 15 min to obtain PMA_{SH}. The polymer was then diluted with NaOAc buffer (20 mM; pH 4) to a final concentration of 2 mg mL^{-1} prior to the assembly of the capsule layers.

Capsule Preparation: Adsorption and Layer-by-Layer. Aminated SiO_2 particles (250 μL, 5 wt %) of 500 nm or 1 μm diameter (MicroParticles GmbH) were washed and dispersed with 125 μL of Tris-EDTA buffer (10 mM; pH 7.5). TAMRA-labeled OVA (125 μL, 0.5 mg mL^{-1}) or a mixture of 0.1 mg mL^{-1} of PMA—$OVA_{257-264}$ and 0.06 mg mL^{-1} of PMA—$OVA_{323-339}$ (125 μL in Tris-EDTA buffer) was added, and adsorption was allowed to proceed for 15 min with constant shaking. The resulting particles were washed with Tris-EDTA buffer and NaOAc buffer (20 mM, pH 4) and finally dispersed in 125 μL of NaOAc buffer. Assembly of the polymer layers was achieved by alternately incubating the particles with 125 μL of PMA_{SH} or poly(vinylpyrrolidone) (PVP, M_W = 10 kDa, 2 mg mL^{-1} in NaOAc buffer) for 15 min at room temperature with constant shaking. The particles were washed with NaOAc buffer (20 mM, pH 4) between layers. The process was repeated until five bilayers of PMA_{SH}/PVP were assembled. To effect oxidation of the thiols into disulfide linkages, the particles were then exposed to a 2.5 mM solution of *N*-chloro-*p*-toluenesulfonamide sodium salt

(chloramine T) in 2-(*N*-morpholine)ethane sulfonic acid (MES) buffer solution (50 mM; pH 6) for 1 min, followed by two washing cycles with MES buffer solution and NaOAc buffer solution (20 mM, pH 4). The silica template was dissolved by treatment with an appropriate amount of aqueous hydrofluoric acid (*Caution! hydrofluoric acid is highly toxic and great care must be taken when handling*), and the obtained capsules were washed with NaOAc buffer (20 mM, pH 4) until the capsules were at pH 4. The use of HF for core dissolution has been used previously without any detrimental effect on biological activity of the encapsulated cargo.[14] Capsules were incubated with 5 mM solution of oxidized L-glutathione (GSSG) for 30−60 min to ensure the removal of PVP and any nonspecifically bound and/or any leaked peptides and subsequently transferred into PBS.

Capsule Characterization. The loading of OVA onto the template particles was determined by incubating 1×10^7 positively charged silica particles (1 μm diameter) with various concentrations of AlexaFluor-488-labeled OVA. The amount of adsorbed OVA was measured by flow cytometry analyses of the particles on a Partec GmbH CyFlow Space flow cytometer. The fluorescence intensity of the supernatant was measured on a HORIBA Jobin Yvon FluoroLog fluorescence spectrometer to determine the amount of OVA remaining in the supernatant. Different OVA concentrations were prepared by diluting a 10 mg mL^{-1} solution of AlexaFluor-488-OVA in TE buffer. For each OVA concentration, six samples were prepared and 1×10^7 silica particles were added to three of the samples, while the remaining samples were used as controls. The particles were incubated in the OVA solution for 1 h and then washed four times with 150 μL of Tris-EDTA buffer. The supernatant from all washes was collected, and control samples were diluted with 600 μL of Tris-EDTA buffer to the same volume. The adsorption efficiency was then calculated by taking the ratio of remaining OVA in solution to the total amount of OVA added. Fully assembled OVA-containing capsules were visualized on a laser-scanning confocal microscope (TCS SP2; Leica, Germany). Cargo release kinetic studies were performed by dispersing the capsules in PBS at pH 7.2 and monitoring the fluorescence intensity in the presence of 5 mM reduced L-glutathione (GSH) at 37 °C at different time points using a BD FACS Calibur flow cytometer. For the purposes of the vaccination experiments, the amount of OVA within the capsules was assumed to be 100% of that in the adsorbing solution.

Mouse Splenocyte and DC Preparation. All mouse experiments were approved by The University of Melbourne Animal Ethics Committee and performed according to national and university guidelines and regulations. All mice were bred and maintained at the Department of Microbiology and Immunology at the University of Melbourne. Single cell suspensions were prepared from the spleens of naïve C57BL/6 mice by collengenase type II (1 mg mL^{-1}, Worthington Biochemicals, USA), DNase I (1 μg mL^{-1}, Boehringer Mannheim, Germany), and EDTA (0.01 M) treatment followed by red blood cell lysis with 8.3 mg mL^{-1} ammonium chloride in 0.01 M Tris-HCl buffer. The splenocyte suspensions were enriched for conventional DCs following a 30 min incubation with antibodies anti-Gr-1 (RB6-8C5), anti-CD3ε (KT3), anti-CD19 (ID6), anti-Thy-1 (T24), anti-B220 (RA3-6B2), and anti-Ter119, by magnetic bead depletion using BioMag goat antirat IgG beads (Qiagen, Australia) as previously described.[28,29]

Binding and Internalization of Capsules by APCs. Splenocytes (1×10^6) were incubated with 1 μm diameter fluorescently labeled OVA-containing PMA_{SH} hydrogel capsules for 1 h at 37 °C with 5% CO_2. Cells were surface stained with anti-CD11b (Mac1, M1/70), anti-CD11c (HL3), anti-B220 (RA3-6B2), and anti-GR1 (RB6-8C5) (all from BD Biosciences, Canada) to identify B cells, neutrophils, and DCs. Binding was assessed by flow cytometry as the percentage of each cell type that had capsule associated fluorescence on a BD LSR-II analyzer and analyzed by FloJo software (version 7.2.2). Internalization was assessed by incubating 1×10^5 enriched splenic DCs with 1 μm diameter fluorescently labeled OVA-loaded capsules for 1 h at 37 °C with 5% CO_2 followed by surface staining with anti-CD11c (HL3; BD Biosciences, Canada) and viewing on a laser-scanning confocal microscope (TCS SP2; Leica, Germany).

***In Vitro* T Cell Stimulation.** Splenocytes (1×10^6) and enriched splenic DCs (1×10^5) were incubated with 1 μm diameter fluorescently labeled OVA-loaded capsules at various capsule to cell ratios for 1 h at 37 °C with 5% CO_2. Meanwhile, CD8 and CD4 T cells were enriched from the lymph nodes of OT-I and OT-II transgenic mice (C57BL/6 background) as previously described.[30] Briefly, T cells were isolated from lymph nodes by incubating with the following antibodies: anti-CD11b (Mac-1, M1/70), anti-F4/80 (F4/80), anti-Ter119, anti-Gr-1 (RB6-8C5), anti-I-A/E (M5114), and either anti-CD4 (GK1.5) for enrichment of CD8 T cells (OT-I) or anti-CD8 (53-6.7) for enrichment of CD4 T cells (OT-II). Cells that bound antibodies were removed by magnetic bead depletion using BioMag goat antirat IgG beads (Qiagen, Australia). Enriched T cells were then labeled by incubation with 5 μM CFSE (5,6-carboxyfluoroscein diacetate succinimidyl ester; Sigma, USA) as previously described.[31] The splenocytes/enriched DCs were washed, and 5×10^4 CFSE-labeled enriched CD4 or CD8 T cells were added before culturing at 37 °C with 5% CO_2 for a further 3 days. After this, T cells were surface stained with anti-CD4 (GK1.5) or anti-CD8 (53.6-7), and anti-Vα2 (B20.1), all from BD Biosciences (Canada), and proliferation of OT-I (CD8+, Vα2+) and OT-II (CD4+, Vα2+) cells was assessed by flow cytometry on a BD FACSCalibur and analyzed by FloJo software (version 7.2.2). Proliferation was measured by the successive halving of the median fluorescence intensity of the CFSE label with each round of replication.

***In Vivo* Stimulation of Adoptively Transferred T Cells.** CD8 and CD4 T cells were enriched from the lymph nodes of CD45-1+ OT-I and OT-II transgenic mice (C57BL/6 background) and CFSE labeled as described above. CD8 (2×10^6) and CD4 (2×10^6) CFSE-labeled enriched T cells were intravenously adoptively transferred into the tail vein of C57BL/6 mice. After 24 h, groups of three mice were vaccinated intravenously *via* the tail vein with either 1×10^9 capsules containing OVA protein/peptides (in 200 μL PBS), soluble OVA protein at an equivalent dose to that inside the capsules (7 μg, in 200 μL PBS), LPS adjuvanted OVA-coated splenocytes (positive control, prepared by incubating naïve splenocytes with 10 mg mL^{-1} OVA and 2 μg mL^{-1} lipopolysaccharide (LPS) at 37 °C for 30 min), or Hanks balanced salt solution (HBSS, negative control). Three days later, the spleen from each mouse was harvested, and cell suspensions were prepared in a final volume of 5 mL by homogenization and red blood cell lysis with 8.3 mg mL^{-1} ammonium chloride in 0.01 M Tris-HCl buffer. An aliquot of splenocytes was surface stained with anti-CD4 (GK1.5), anti-CD8 (53.6-7), anti-Vα2 (B20.1), and anti-CD45-1 (A20), all from BD Biosciences (Canada), and proliferation of the adoptively transferred T cells was measured by the successive halving of the median fluorescence intensity of the CFSE label by flow cytometery on a BD FACSCanto II and analyzed by FloJo software (version 7.2.2).

Acknowledgment. We thank staff at the Microbiology and Immunology animal facility at The University of Melbourne. This work is supported by National Health and Medical Research Council grants (S.J.K.), Australian Research Council grants under the Federation Fellowship (F.C.) and Discovery Project (F.C., A.P.R.J., A.N.Z.) schemes, and The University of Melbourne Strategic Research Infrastructure Fund (F.C., S.J.K.).

REFERENCES AND NOTES

1. Koup, R. A.; Safrit, J. T.; Cao, Y.; Andrews, C. A.; McLeod, G.; Borkowsky, W.; Farthing, C.; Ho, D. D. Temporal Association of Cellular Immune Responses with the Initial Control of Viremia in Primary Human Immunodeficiency Virus Type 1 Syndrome. *J. Virol.* **1994**, *68*, 4650–4655.
2. Altfeld, M.; Rosenberg, E. S. The Role of CD4+ T Helper Cells in the Cytotoxic T Lymphocyte Response to HIV-1. *Curr. Opin. Immunol.* **2000**, *12*, 375–380.
3. Kalams, S. A.; Walker, B. D. The Critical Need for CD4 Help in Maintaining Effective Cytotoxic T Lymphocyte Responses. *J. Exp. Med.* **1998**, *188*, 2199–2204.
4. Grakoui, A.; Shoukry, N. H.; Woollard, D. J.; Man, J.-H.; Hanson, H. L.; Ghrayeb, J.; Murthy, K. K.; Rice, C. M.; Walker,

C. M. HCV Persistence and Immune Evasion in the Absence of Memory T Cell Help. *Science* **2003**, *302*, 659–662.
5. De Rose, R.; Fernandez, C. S.; Smith, M. Z.; Batten, C. J.; Alcantara, S.; Peut, V.; Rollman, E.; Loh, L.; Mason, R. D.; Wilson, K.; Law, M. G.; Handley, A. J.; Kent, S. J. Control of Viremia and Prevention of AIDS Following Immunotherapy of SIV-Infected Macaques with Peptide-Pulsed Blood. *PLoS Pathog.* **2008**, *4*, e1000055.
6. Neundorf, I.; Rennert, R.; Franke, J.; Kozle, I.; Bergmann, R. Detailed Analysis Concerning the Biodistribution and Metabolism of Human Calcitonin-Derived Cell-Penetrating Peptides. *Bioconjugate Chem.* **2008**, *19*, 1596–1603.
7. Kataoka, K.; Harada, A.; Nagasaki, Y. Block Copolymer Micelles for Drug Delivery: Design, Characterization and Biological Significance. *Adv. Drug Delivery Rev.* **2001**, *47*, 113–131.
8. Torchilin, V. P. Recent Advances with Liposomes as Pharmaceutical Carriers. *Nat. Rev. Drug Discovery* **2005**, *4*, 145–160.
9. Discher, D. E.; Ahmed, F. Polymersomes. *Annu. Rev. Biomed. Eng.* **2006**, *8*, 323–341.
10. Lensen, D.; Vriezema, D. M.; van Hest, J. C. Polymeric Microcapsules for Synthetic Applications. *Macromol. Biosci.* **2008**, *8*, 991–1005.
11. Donath, E.; Sukhorukov, G. B.; Caruso, F.; Davis, S. A.; Mohwald, H. Novel Hollow Polymer Shells by Colloid-Templated Assembly of Polyelectrolytes. *Angew. Chem., Int. Ed.* **1998**, *37*, 2201–2205.
12. Caruso, F.; Caruso, R. A.; Möhwald, H. Nanoengineering of Inorganic and Hybrid Hollow Spheres by Colloidal Templating. *Science* **1998**, *282*, 1111.
13. De Rose, R.; Zelikin, A. N.; Johnston, A. P. R.; Sexton, A.; Chong, S.-F.; Cortez, C.; Mulholland, W.; Caruso, F.; Kent, S. J. Binding, Internalization, and Antigen Presentation of Vaccine-Loaded Nanoengineered Capsules in Blood. *Adv. Mater.* **2008**, *20*, 4698–4703.
14. Chong, S.-F.; Sexton, A.; De Rose, R.; Kent, S. J.; Zelikin, A. N.; Caruso, F. A Paradigm for Peptide Vaccine Delivery Using Viral Epitopes Encapsulated in Degradable Polymer Hydrogel Capsules. *Biomaterials* **2009**, *30*, 5178–5186.
15. Nayak, J. V.; Hokey, D. A.; Larregina, A.; He, Y.; Salter, R. D.; Watkins, S. C.; Falo, L. D., Jr. Phagocytosis Induces Lysosome Remodeling and Regulated Presentation of Particulate Antigens by Activated Dendritic Cells. *J. Immunol.* **2006**, *177*, 8493–8503.
16. Zelikin, A. N.; Quinn, J. F.; Caruso, F. Disulfide Cross-Linked Polymer Capsules: *En Route* to Biodeconstructible Systems. *Biomacromolecules* **2006**, *7*, 27–30.
17. Zelikin, A. N.; Li, Q.; Caruso, F. Disulfide-Stabilized Poly(methacrylic acid) Capsules: Formation, Cross-Linking, and Degradation Behavior. *Chem. Mater.* **2008**, *20*, 2655–2661.
18. Clarke, S. R.; Barnden, M.; Kurts, C.; Carbone, F. R.; Miller, J. F.; Heath, W. R. Characterization of the Ovalbumin-Specific TCR Transgenic Line OT-I: MHC Elements for Positive and Negative Selection. *Immunol. Cell. Biol.* **2000**, *78*, 110–117.
19. Barnden, M. J.; Allison, J.; Heath, W. R.; Carbone, F. R. Defective TCR Expression in Transgenic Mice Constructed Using cDNA-Based Alpha- and Beta-Chain Genes under the Control of Heterologous Regulatory Elements. *Immunol. Cell. Biol.* **1998**, *76*, 34–40.
20. Sivakumar, S.; Bansal, V.; Cortez, C.; Chong, S.-F.; Zelikin, A. N.; Caruso, F. Degradable, Surfactant-Free, Monodisperse Polymer-Encapsulated Emulsions as Anticancer Drug Carriers. *Adv. Mater.* **2009**, *21*, 1820–1824.
21. Zelikin, A. N.; Becker, A. L.; Johnston, A. P. R.; Wark, K. L.; Turatti, F.; Caruso, F. A General Approach for DNA Encapsulation in Degradable Polymer Microcapsules. *ACS Nano* **2007**, *1*, 63–69.
22. Wang, Y.; Caruso, F. Mesoporous Silica Spheres as Supports for Enzyme Immobilization and Encapsulation. *Chem. Mater.* **2005**, *17*, 953–961.
23. Saric, T.; Beninga, J.; Graef, C. I.; Akopian, T. N.; Rock, K. L.; Goldberg, A. L. Major Histocompatibility Complex Class I-Presented Antigenic Peptides are Degraded in Cytosolic Extracts Primarily by Thimet Oligopeptidase. *J. Biol. Chem.* **2001**, *276*, 36474–36481.
24. Zhang, X.-Q.; Dahle, C. E.; Weiner, G. J.; Salem, A. K. A. Comparative Study of the Antigen-Specific Immune Response Induced by Co-delivery of CpG ODN and Antigen Using Fusion Molecules or Biodegradable Microparticles. *J. Pharm. Sci.* **2007**, *96*, 3283–3292.
25. Standley, S. M.; Mende, I.; Goh, S. L.; Kwon, Y. J.; Beaudette, T. T.; Engleman, E. G.; Frechet, J. M. J. Incorporation of CpG Oligonucleotide Ligand into Protein-Loaded Particle Vaccines Promotes Antigen-Specific CD8 T-Cell Immunity. *Bioconjugate Chem.* **2006**, *18*, 77–83.
26. Quinn, J. F.; Johnston, A. P.; Such, G. K.; Zelikin, A. N.; Caruso, F. Next Generation, Sequentially Assembled Ultrathin Films: Beyond Electrostatics. *Chem. Soc. Rev.* **2007**, *36*, 707–718.
27. Werle, M.; Hoffer, M. Glutathione and Thiolated Chitosan Inhibit Multidrug Resistance P-Glycoprotein Activity in Excised Small Intestine. *J. Controlled Release* **2006**, *111*, 41–46.
28. Allan, R. S.; Waithman, J.; Bedoui, S.; Jones, C. M.; Villadangos, J. A.; Zhan, Y.; Lew, A. M.; Shortman, K.; Heath, W. R.; Carbone, F. R. Migratory Dendritic Cells Transfer Antigen to a Lymph Node-Resident Dendritic Cell Population for Efficient CTL Priming. *Immunity* **2006**, *25*, 153–162.
29. Belz, G. T.; Bedoui, S.; Kupresanin, F.; Carbone, F. R.; Heath, W. R. Minimal Activation of Memory CD8+ T Cell by Tissue-Derived Dendritic Cells Favors the Stimulation of Naive CD8+ T Cells. *Nat. Immunol.* **2007**, *8*, 1060–1066.
30. Bedoui, S.; Whitney, P. G.; Waithman, J.; Eidsmo, L.; Wakim, L.; Caminschi, I.; Allan, R. S.; Wojtasiak, M.; Shortman, K.; Carbone, F. R.; Brooks, A. G.; Heath, W. R. Cross-Presentation of Viral and Self Antigens by Skin-Derived CD103+ Dendritic Cells. *Nat. Immunol.* **2009**, *10*, 488–495.
31. Kurts, C.; Kosaka, H.; Carbone, F. R.; Miller, J. F.; Heath, W. R. Class I-Restricted Cross-Presentation of Exogenous Self-Antigens Leads to Deletion of Autoreactive CD8(+) T Cells. *J. Exp. Med.* **1997**, *186*, 239–245.